Available online at www.sciencedirect.com
SCIENCE DIRECT®
International Journal of Solids and Structures 43 (2006) 5196–5216
INTERNATIONAL JOURNAL OF SOLIDS and STRUCTURES
www.elsevier.com/locate/ijsolstr

Dynamic internal crack problem of a functionally graded magneto-electro-elastic strip

W.J. Feng [a], R.K.L. Su [b,*]

[a] Department of Mechanics and Engineering Science, Shijiazhuang Railway Institute, Shijiazhuang 050043, PR China
[b] Department of Civil Engineering, The University of Hong Kong, Hong Kong, PR China

Received 19 April 2005; received in revised form 20 July 2005
Available online 21 September 2005

Abstract

In this paper the dynamic anti-plane problem for a functionally graded magneto-electro-elastic strip containing an internal crack perpendicular to the boundary is investigated. The crack is assumed to be either magneto-electrically impermeable or permeable. Integral transforms and dislocation density functions are employed to reduce the problem to Cauchy singular integral equations. Numerical results show the effects of loading combination parameter, material gradient parameter and crack configuration on the dynamic response. With the magneto-electrically permeable assumption, both the magnetical and electrical impacts have no contribution to the crack tip field singularity. However, with the impermeable assumption, both the applied magnetical loads and electrical loads play a dominant role in the dynamic fracture behavior of crack tips. And for the two kinds of crack surface conditions, increasing the graded index can all retard the crack extension.

Keywords: Impact; Magneto-electro-elastic material; Functionally graded material (FGM); Crack; Dynamic energy release rate; Singular integral equation; Integral transform; Strip

1. Introduction

Composite material consisting of a piezoelectric phase and a piezomagnetic phase has drawn significant interest in recent years, due to the rapid development and application of this material in adaptive

* Corresponding author. Tel.: +85 228592648; fax: +85 225595337.
E-mail addresses: fengwj@sjzri.edu.cn (W.J. Feng), klsu@hkucc.hku.hk (R.K.L. Su).

0020-7683/$ - see front matter
doi:10.1016/j.ijsolstr.2005.07.050

control systems. It shows a remarkably large magnetoelectric coefficient, the coupling coefficient between static electric and magnetic fields, which does not exist in either component. The magnetoelectric coupling is a new product property of the composite, since it is absent in each component. In some cases, the coupling effect of piezoelectric/piezomagnetic composites can be even a hundred times larger than that in a single-phase magnetoelectric material. Consequently, they are extensively used as magnetic field probes, electric packaging, acoustic, hydrophones, medical ultrasonic imaging, sensors, and actuators with the functionality of magneto-electro-mechanical energy conversion (Wu and Huang, 2000). When subjected to mechanical, magnetical and electrical loads in service, these magneto-electro-elastic composites can fail prematurely due to some defects, such as cracks, holes and inclusions arising during their manufacturing process. Therefore, it is of great importance to study the fracture behaviors of piezoelectric/piezomagnetic composites under magneto-electro-elastic interactions (Song and Sih, 2003; Sih and Song, 2003).

The development of piezoelectric-piezomagnetic composites has its root from the early work of Van Suchtelen (1972) who proposed that the combination of piezoelectric-piezomagnetic phases might exhibit a new material property—the magnetoelectric coupling effect. Since then, the magnetoelectric coupling effect of $BaTiO_3$-$CoFe_2O_4$ composites has been measured by many researchers. Much of the theoretical work for the investigation of magneto-electro-elastic coupling effect has only recently been studied (Wu and Huang, 2000; Song and Sih, 2003; Sih and Song, 2003; Harshe et al., 1993; Avellaneda and Harshe, 1994; Nan, 1994; Benveniste, 1995; Wang and Shen, 1996; Huang and Kuo, 1997; Li and Dunn, 1998; Li, 2000; Pan, 2001; Zhou et al., 2004; Lage et al., 2004).

To date, analysis of dynamic fracture problems of magneto-electro-elastic material is very limited. Du et al. (2004) obtained the scattered fields of SH waves by a partially debonded magneto-electro-elastic cylindrical inhomogeneity, and determined the numerical results of crack opening displacement. Hou and Leung (2004) analyzed the plane strain dynamic problem of a magneto-electro-elastic hollow cylinder by virtue of the separation of variables, orthogonal expansion technique and the interpolation method. Buchanan (2003) considered the free vibration problem of an infinite magneto-electro-elastic cylinder. To the best of our knowledge, in all of these studies, the magneto-electro-elastic media are either homogeneous or multi-layered.

On the other hand, although the transient response of piezoelectric material with cracks are widely investigated (Shindo et al., 1996; Chen and Yu, 1997; Wang and Yu, 2000; Kwon and Lee, 2000; Li, 2001; Gu et al., 2002; Chen et al., 2003), to our knowledge, the transient response of cracks in magneto-electro-elastic media has not been studied.

In this paper, the dynamic anti-plane problem of a functionally graded magneto-electro-elastic strip containing an internal crack perpendicular to the boundary is studied. The material properties are assumed to vary exponentially along the x-direction. Two kinds of crack surface conditions, i.e. magneto-electrically impermeable and magneto-electrically permeable, are adopted. Integral transform technique is used to reduce the problem to the solution of singular integral equations. Numerical results are shown graphically to illustrate the effects of loading combination parameter, material gradient parameter and crack configuration on the dynamic responses.

2. Statement of problem

Consider an infinite magneto-electro-elastic strip that contains a Griffith crack with reference to the rectangular coordinate system x, y, z, as shown in Fig. 1. The strip exhibits transversely isotropic behavior and is poled in z-direction. The anti-plane shear impacts and in-plane electric displacement and magnetic induction impacts are suddenly applied on the crack surfaces at $t = 0$, and then maintain constants as imposed loads. In Fig. 1, $H(t)$ denotes the Heaviside unit step function.

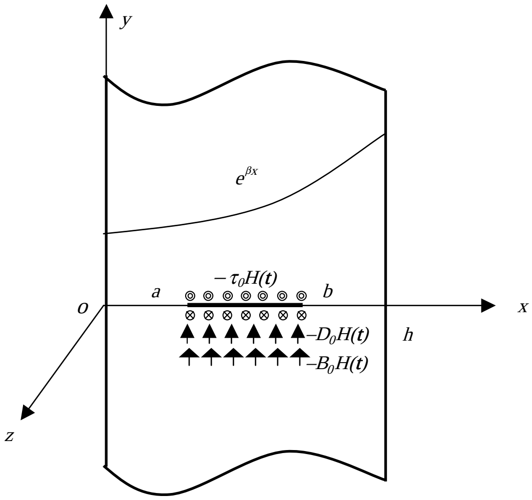

Fig. 1. Crack problem for a functionally graded magneto-electro-elastic strip.

The constitutive equations for anti-plane magneto-electro-elastic media can be written as:

$$\sigma_{zx} = c_{44}\frac{\partial w}{\partial x} + e_{15}\frac{\partial \phi}{\partial x} + f_{15}\frac{\partial \psi}{\partial x}, \quad \sigma_{zy} = c_{44}\frac{\partial w}{\partial y} + e_{15}\frac{\partial \phi}{\partial y} + f_{15}\frac{\partial \psi}{\partial y}, \tag{1}$$

$$D_x = e_{15}\frac{\partial w}{\partial x} - \varepsilon_{11}\frac{\partial \phi}{\partial x} - g_{11}\frac{\partial \psi}{\partial x}, \quad D_y = e_{15}\frac{\partial w}{\partial y} - \varepsilon_{11}\frac{\partial \phi}{\partial y} - g_{11}\frac{\partial \psi}{\partial y}, \tag{2}$$

$$B_x = f_{15}\frac{\partial w}{\partial x} - g_{11}\frac{\partial \phi}{\partial x} - \mu_{11}\frac{\partial \psi}{\partial x}, \quad B_y = f_{15}\frac{\partial w}{\partial y} - g_{11}\frac{\partial \phi}{\partial y} - \mu_{11}\frac{\partial \psi}{\partial y}, \tag{3}$$

where σ_{zk}, D_k, B_k $(k = x, y)$ are the anti-plane shear stress, in-plane electric displacement and magnetic induction, respectively; c_{44}, ε_{11}, e_{15}, f_{15}, g_{11}, μ_{11} are the material constants; w, ϕ and ψ are the mechanical displacement, electric potential and magnetic potential, respectively.

The material properties are assumed to be one-dimensionally dependent as:

$$c_{44} = c_{440}\mathrm{e}^{\beta x}, \quad \varepsilon_{11} = \varepsilon_{110}\mathrm{e}^{\beta x}, \quad e_{15} = e_{150}\mathrm{e}^{\beta x}, \quad f_{15} = f_{150}\mathrm{e}^{\beta x}, \quad g_{11} = g_{110}\mathrm{e}^{\beta x}, \quad \mu_{11} = \mu_{110}\mathrm{e}^{\beta x}, \quad \rho = \rho_0\mathrm{e}^{\beta x}, \tag{4}$$

where ρ is the mass density.

Substituting Eqs. (1)–(3) into the basic equations of magneto-electro-elastic boundary value problem, i.e.,

$$\frac{\partial \sigma_{zx}}{\partial x} + \frac{\partial \sigma_{zy}}{\partial y} = \rho\frac{\partial^2 w}{\partial t^2}, \tag{5}$$

$$\frac{\partial D_x}{\partial x} + \frac{\partial D_y}{\partial y} = 0, \tag{6}$$

$$\frac{\partial B_x}{\partial x} + \frac{\partial B_y}{\partial y} = 0 \tag{7}$$

and applying Eq. (4), we can obtain the governing equation as follows:

$$c_{440}\left(\nabla^2 w+\beta\frac{\partial w}{\partial x}\right)+e_{150}\left(\nabla^2\phi+\beta\frac{\partial\phi}{\partial x}\right)+f_{150}\left(\nabla^2\psi+\beta\frac{\partial\psi}{\partial x}\right)=\rho_0\frac{\partial^2 w}{\partial t^2}, \tag{8}$$

$$e_{150}\left(\nabla^2 w+\beta\frac{\partial w}{\partial x}\right)-\varepsilon_{110}\left(\nabla^2\phi+\beta\frac{\partial\phi}{\partial x}\right)-g_{110}\left(\nabla^2\psi+\beta\frac{\partial\psi}{\partial x}\right)=0, \tag{9}$$

$$f_{150}\left(\nabla^2 w+\beta\frac{\partial w}{\partial x}\right)-g_{110}\left(\nabla^2\phi+\beta\frac{\partial\phi}{\partial x}\right)-\mu_{110}\left(\nabla^2\psi+\beta\frac{\partial\psi}{\partial x}\right)=0, \tag{10}$$

where $\nabla^2=\partial^2/\partial x^2+\partial^2/\partial y^2$ is the two-dimensional Laplace operator.

Assume

$$\phi=d_1w+e_1\chi+f_1\zeta,\quad \psi=d_2w+e_2\chi+f_2\zeta, \tag{11}$$

where d_1, e_1, f_1, d_2, e_2 and f_2 (referring to Appendix A) are the known constants. The governing Eqs. (8)–(10) can be expressed as:

$$\nabla^2 w+\beta\frac{\partial w}{\partial x}=c_2^{-2}\frac{\partial^2 w}{\partial t^2}, \tag{12}$$

$$\nabla^2\chi+\beta\frac{\partial\chi}{\partial x}=0, \tag{13}$$

$$\nabla^2\zeta+\beta\frac{\partial\zeta}{\partial x}=0, \tag{14}$$

where $c_2=\sqrt{\mu_0/\rho_0}$ is the shear wave speed and

$$\mu_0=c_{440}+\frac{e_{150}^2\mu_{110}-2e_{150}f_{150}g_{110}+f_{150}^2\varepsilon_{110}}{\mu_{110}\varepsilon_{110}-g_{150}^2}. \tag{15}$$

The constitutive relations (1)–(3) can be rewritten as:

$$\sigma_{zx}=e^{\beta x}\left(m_{10}w_{,x}+m_{20}\chi_{,x}+m_{30}\zeta_{,x}\right),\quad \sigma_{zy}=e^{\beta x}\left(m_{10}w_{,y}+m_{20}\chi_{,y}+m_{30}\zeta_{,y}\right), \tag{16}$$

$$D_x=e^{\beta x}\chi_{,x},\quad D_y=e^{\beta x}\chi_{,y}, \tag{17}$$

$$B_x=e^{\beta x}\zeta_{,x}\quad B_y=e^{\beta x}\zeta_{,y}, \tag{18}$$

where m_{10}, m_{20} and m_{30} refer to Appendix A as well.

For the magneto-electrically impermeable crack, the boundary conditions are

$$\sigma_{zx}(0,y,t)=D_x(0,y,t)=B_x(0,y,t)=0,\quad -\infty<y<\infty, \tag{19}$$

$$\sigma_{zx}(h,y,t)=D_x(h,y,t)=B_x(h,y,t)=0,\quad -\infty<y<\infty, \tag{20}$$

$$\sigma_{zy}(x,0,t)=-\tau_0H(t),\quad D_y(x,0,t)=-D_0H(t),\quad B_y(x,0,t)=-B_0H(t),\quad x\in(a,b), \tag{21}$$

$$w(x,0,t)=\phi(x,0,t)=\psi(x,0,t)=0,\quad x\notin(a,b). \tag{22}$$

For the magneto-electrically permeable case, the boundary conditions are

$$\sigma_{zx}(0,y,t)=D_x(0,y,t)=B_x(0,y,t)=0,\quad -\infty<y<\infty, \tag{23}$$

$$\sigma_{zx}(h,y,t)=D_x(h,y,t)=B_x(h,y,t)=0,\quad -\infty<y<\infty, \tag{24}$$

$$\sigma_{zy}(x,0,t)=-\tau_0H(t),\quad x\in(a,b), \tag{25}$$

$$w(x,0,t)=0,\quad x\notin(a,b), \tag{26}$$

$$\phi(x,0,t)=\psi(x,0,t)=0,\quad x\in(0,h). \tag{27}$$

And the electric displacement $D_y(x, 0, t)$ and magnetic induction $B_y(x, 0, t)$ on the crack surfaces consist of two components. The first is the imposed electric displacement $-D_0H(t)$ and magnetic induction $-B_0H(t)$ for $D_y(x, 0, t)$ and $B_y(x, 0, t)$, respectively. The second is the unknown caused by $-\tau_0H(t)$ for both of $D_y(x, 0, t)$ and $B_y(x, 0, t)$.

3. Derivation and solution of singular integral equations

We proceed with the magneto-electrically impermeable case. Define a Laplace transform pair as:

$$f^*(p) = \int_0^\infty f(t)\mathrm{e}^{-pt}\,\mathrm{d}t, \quad f(t) = \frac{1}{2\pi \mathrm{i}}\int_{Br} f^*(p)\mathrm{e}^{pt}\,\mathrm{d}p, \tag{28}$$

in which Br stands for the Bromwich path of integration. The time-dependence in Eqs. (12)–(14) are eliminated by the application of Eq. (28). Employing the Fourier transform on the variable x and the Fourier sine transform on the variable y and noting at infinity the quantities in the left side of Eqs. (12)–(14) must be limited, we obtain

$$w^*(x,y,p) = \frac{1}{2\pi}\int_{-\infty}^{+\infty} A_1(\alpha,p)\mathrm{e}^{-m_1 y}\mathrm{e}^{-\mathrm{i}\alpha x}\,\mathrm{d}\alpha + \frac{2}{\pi}\int_0^\infty \sum_{j=2}^{3} A_j(\alpha,p)\mathrm{e}^{m_j x}\sin(\alpha y)\,\mathrm{d}\alpha, \tag{29}$$

$$\chi^*(x,y,p) = \frac{1}{2\pi}\int_{-\infty}^{+\infty} B_1(\alpha,p)\mathrm{e}^{-n_1 y}\mathrm{e}^{-\mathrm{i}\alpha x}\,\mathrm{d}\alpha + \frac{2}{\pi}\int_0^\infty \sum_{j=2}^{3} B_j(\alpha,p)\mathrm{e}^{n_j x}\sin(\alpha y)\,\mathrm{d}\alpha, \tag{30}$$

$$\zeta^*(x,y,p) = \frac{1}{2\pi}\int_{-\infty}^{+\infty} C_1(\alpha,p)\mathrm{e}^{-n_1 y}\mathrm{e}^{-\mathrm{i}\alpha x}\,\mathrm{d}\alpha + \frac{2}{\pi}\int_0^\infty \sum_{j=2}^{3} C_j(\alpha,p)\mathrm{e}^{n_j x}\sin(\alpha y)\,\mathrm{d}\alpha, \tag{31}$$

where A_j, B_j, C_j ($j = 1, 2, 3$) are the unknowns to be solved and

$$m_1(\alpha,p) = \sqrt{\alpha^2 + p^2/c_2^2 + \mathrm{i}\beta\alpha}, \quad m_{2,3}(\alpha,p) = -\beta/2 \mp \sqrt{\beta^2/4 + \alpha^2 + p^2/c_2^2}, \tag{32a}$$

$$n_1(\alpha) = \sqrt{\alpha^2 + \mathrm{i}\beta\alpha}, \quad n_{2,3}(\alpha) = -\beta/2 \mp \sqrt{\beta^2/4 + \alpha^2}. \tag{32b}$$

Defining dislocation density functions $g_i(x, p)$, $i = 1, 2, 3$, as follows

$$g_1(x,p) = \frac{\partial w^*(x,0,p)}{\partial x}, \quad g_2(x,p) = \frac{\partial \phi^*(x,0,p)}{\partial x}, \quad g_3(x,p) = \frac{\partial \psi^*(x,0,p)}{\partial x}, \quad x \in (a,b), \tag{33a}$$

$$g_1(x,p) = g_2(x,p) = g_3(x,p) = 0, \quad x \notin (a,b), \tag{33b}$$

and applying Eqs. (29)–(31) and Eq. (11), we obtain

$$A_1 = \frac{\mathrm{i}}{\alpha}\int_a^b g_1(u,p)\mathrm{e}^{\mathrm{i}\alpha u}\,\mathrm{d}u, \tag{34}$$

$$B_1 = \frac{\mathrm{i}}{\alpha}\int_a^b g_{123}^{e\varepsilon g}(u,p)\mathrm{e}^{\mathrm{i}\alpha u}\,\mathrm{d}u, \tag{35}$$

$$C_1 = \frac{\mathrm{i}}{\alpha}\int_a^b g_{123}^{fg\mu}(u,p)\mathrm{e}^{\mathrm{i}\alpha u}\,\mathrm{d}u, \tag{36}$$

where

$$g_{123}^{e\varepsilon g} = e_{150}g_1(u,p) - \varepsilon_{110}g_2(u,p) - g_{110}g_3(u,p), \tag{37a}$$

$$g_{123}^{fg\mu} = f_{150}g_1(u,p) - g_{110}g_2(u,p) - \mu_{110}g_3(u,p). \tag{37b}$$

Similarly, using Eqs. (16)–(18), (29)–(31), (34)–(36), together with the boundary conditions (19) and (20), it follows that

$$A_2 m_2 + A_3 m_3 = \int_a^b g_1(u,p) F_1(\alpha,u,p)\,\mathrm{d}u, \tag{38}$$

$$B_2 n_2 + B_3 n_3 = \int_a^b g_{123}^{e\varepsilon g}(u,p) F_2(\alpha,u)\,\mathrm{d}u, \tag{39}$$

$$C_2 n_2 + C_3 n_3 = \int_a^b g_{123}^{fg\mu}(u,p) F_2(\alpha,u)\,\mathrm{d}u, \tag{40}$$

$$A_2 m_2 \mathrm{e}^{m_2 h} + A_3 m_3 \mathrm{e}^{m_3 h} = \int_a^b g_1(u,p) F_4(\alpha,u,p)\,\mathrm{d}u, \tag{41}$$

$$B_2 n_2 \mathrm{e}^{n_2 h} + B_3 n_3 \mathrm{e}^{n_3 h} = \int_a^b g_{123}^{e\varepsilon g}(u,p) F_5(\alpha,u)\,\mathrm{d}u, \tag{42}$$

$$C_2 n_2 \mathrm{e}^{n_2 h} + C_3 n_3 \mathrm{e}^{n_3 h} = \int_a^b g_{123}^{fg\mu}(u,p) F_5(\alpha,u)\,\mathrm{d}u, \tag{43}$$

where

$$F_1 = \frac{1}{2\pi}\int_{-\infty}^{\infty} \frac{-\alpha}{m_1^2(\rho,p)+\alpha^2}\mathrm{e}^{\mathrm{i}\rho u}\,\mathrm{d}\rho, \quad F_2 = \frac{1}{2\pi}\int_{-\infty}^{\infty} \frac{-\alpha}{n_1^2(\rho)+\alpha^2}\mathrm{e}^{\mathrm{i}\rho u}\,\mathrm{d}\rho, \tag{44a}$$

$$F_4 = \frac{1}{2\pi}\int_{-\infty}^{\infty} \frac{-\alpha}{m_1^2(\rho,p)+\alpha^2}\mathrm{e}^{-\mathrm{i}\rho(h-u)}\,\mathrm{d}\rho, \quad F_5 = \frac{1}{2\pi}\int_{-\infty}^{\infty} \frac{-\alpha}{n_1^2(\rho)+\alpha^2}\mathrm{e}^{-\mathrm{i}\rho(h-u)}\,\mathrm{d}\rho. \tag{44b}$$

By using the theory of residues, the integrals in Eq. (44) may be evaluated as follows:

$$F_1 = \frac{\alpha \mathrm{e}^{-um_3(\alpha,p)}}{m_2(\alpha,p)-m_3(\alpha,p)}, \quad F_2 = \frac{\alpha \mathrm{e}^{-un_3(\alpha)}}{n_2(\alpha)-n_3(\alpha)}, \tag{45a}$$

$$F_4 = \frac{\alpha \mathrm{e}^{(h-u)m_2(\alpha,p)}}{m_2(\alpha,p)-m_3(\alpha,p)}, \quad F_5 = \frac{\alpha \mathrm{e}^{(h-u)n_2(\alpha)}}{n_2(\alpha)-n_3(\alpha)}. \tag{45b}$$

Noting Eq. (45), A_2, A_3, B_2, B_3, C_2, C_3 can be expressed from (38)–(43) as

$$A_2 = \frac{1}{(\mathrm{e}^{m_2 h}-\mathrm{e}^{m_3 h})m_2}\int_a^b [F_4(\alpha,u,p) - \mathrm{e}^{m_3 h}F_1(\alpha,u,p)] g_1(u,p)\,\mathrm{d}u, \tag{46}$$

$$A_3 = \frac{1}{(\mathrm{e}^{m_2 h}-\mathrm{e}^{m_3 h})m_3}\int_a^b [\mathrm{e}^{m_2 h}F_1(\alpha,u,p) - F_4(\alpha,u,p)] g_1(u,p)\,\mathrm{d}u, \tag{47}$$

$$B_2 = \frac{1}{(\mathrm{e}^{n_2 h}-\mathrm{e}^{n_3 h})n_2}\int_a^b [F_5(\alpha,u) - \mathrm{e}^{n_3 h}F_2(\alpha,u)] g_{123}^{e\varepsilon g}(u,p)\,\mathrm{d}u, \tag{48}$$

$$B_3 = \frac{1}{(\mathrm{e}^{n_2 h}-\mathrm{e}^{n_3 h})n_3}\int_a^b [\mathrm{e}^{n_2 h}F_2(\alpha,u) - F_5(\alpha,u)] g_{123}^{e\varepsilon g}(u,p)\,\mathrm{d}u, \tag{49}$$

$$C_2 = \frac{1}{(\mathrm{e}^{n_2 h}-\mathrm{e}^{n_3 h})n_2}\int_a^b [F_5(\alpha,u) - \mathrm{e}^{n_3 h}F_2(\alpha,u)] g_{123}^{fg\mu}(u,p)\,\mathrm{d}u, \tag{50}$$

$$C_3 = \frac{1}{(\mathrm{e}^{n_2 h}-\mathrm{e}^{n_3 h})n_3}\int_a^b [\mathrm{e}^{n_2 h}F_2(\alpha,u) - F_5(\alpha,u)] g_{123}^{fg\mu}(u,p)\,\mathrm{d}u. \tag{51}$$

Substituting Eqs. (29)–(31) into Eqs. (16)–(18) in Laplace transform domain, we obtain

$$\sigma^*_{zy}(x,0,p) = \mathrm{e}^{\beta x}\left[\frac{1}{2\pi}\int_{-\infty}^{\infty} -(m_{10}m_1A_1 + m_{20}n_1B_1 + m_{30}n_1C_1)\mathrm{e}^{-\mathrm{i}\alpha x}\,\mathrm{d}\alpha + \frac{2}{\pi}\int_0^{\infty}\sum_{j=2}^{3}\left(m_{10}A_j\mathrm{e}^{m_jx} + m_{20}B_j\mathrm{e}^{n_jx} + m_{30}C_j\mathrm{e}^{n_jx}\right)\alpha\,\mathrm{d}\alpha\right], \tag{52}$$

$$D^*_y(x,0,p) = \mathrm{e}^{\beta x}\left[\frac{1}{2\pi}\int_{-\infty}^{\infty} -n_1B_1\mathrm{e}^{-\mathrm{i}\alpha x}\,\mathrm{d}\alpha + \frac{2}{\pi}\int_0^{\infty}\sum_{j=2}^{3}(B_j\mathrm{e}^{n_jx})\alpha\,\mathrm{d}\alpha\right], \tag{53}$$

$$B^*_y(x,0,p) = \mathrm{e}^{\beta x}\left[\frac{1}{2\pi}\int_{-\infty}^{\infty} -n_1C_1\mathrm{e}^{-\mathrm{i}\alpha x}\,\mathrm{d}\alpha + \frac{2}{\pi}\int_0^{\infty}\sum_{j=2}^{3}(C_j\mathrm{e}^{n_jx})\alpha\,\mathrm{d}\alpha\right]. \tag{54}$$

By means of Eqs. (34)–(37), (46)–(54) and boundary conditions (21) in Laplace transform domain, we can obtain the following integral equations:

$$\frac{1}{\pi}\int_a^b\left\{\left[m_{10}(h_{11}+\tilde{h}_{11}) + (\varepsilon_{110}f_{150}^2 - 2e_{150}f_{150}g_{110} + \mu_{110}e_{150}^2)/(g_{110}^2 - \varepsilon_{110}\mu_{110})(h_{12}+\tilde{h}_{12})\right] g_1(u,p) + e_{150}(h_{12}+\tilde{h}_{12})g_2(u,p) + f_{150}(h_{12}+\tilde{h}_{12})g_3(u,p)\right\}\mathrm{d}u = -\tau_0\mathrm{e}^{-\beta x}/p, \quad x\in(a,b), \tag{55}$$

$$\frac{1}{\pi}\int_a^b\left[e_{150}(h_{12}+\tilde{h}_{12})g_1(u,p) - \varepsilon_{110}(h_{12}+\tilde{h}_{12})g_2(u,p) - g_{110}(h_{12}+\tilde{h}_{12})g_3(u,p)\right]\mathrm{d}u = -D_0\mathrm{e}^{-\beta x}/p, \quad x\in(a,b), \tag{56}$$

$$\frac{1}{\pi}\int_a^b\left[f_{150}(h_{12}+\tilde{h}_{12})g_1(u,p) - g_{110}(h_{12}+\tilde{h}_{12})g_2(u,p) - \mu_{110}(h_{12}+\tilde{h}_{12})g_3(u,p)\right]\mathrm{d}u = -B_0\mathrm{e}^{-\beta x}/p, \quad x\in(a,b), \tag{57}$$

where $h_{11}(u,x,p)$, $h_{12}(u,x)$, $\tilde{h}_{11}(u,x,p)$ and $\tilde{h}_{12}(u,x)$ (given in Appendix B) are the known functions.

Following the method developed by Erdogan and Gupta (1972), Eqs. (55)–(57) can be modified as follows:

$$\frac{1}{\pi}\int_a^b\left\{\left[m_{10}(h_{11}+\tilde{k}_{11}-Q) + c_{440}\left(\frac{1}{u-x}+Q\right)\right]g_1(u,p) + e_{150}\left(\frac{1}{u-x}+Q\right)g_2(u,p) + \left(\frac{1}{u-x}+Q\right)f_{150}g_3(u,p)\right\}\mathrm{d}u = -\frac{\tau_0}{p}\mathrm{e}^{-\beta x}, \quad x\in(a,b), \tag{58}$$

$$\frac{1}{\pi}\int_a^b\left[e_{150}\left(\frac{1}{u-x}+Q\right)g_1(u,p) - \varepsilon_{110}\left(\frac{1}{u-x}+Q\right)g_2(u,p) - g_{110}\left(\frac{1}{u-x}+Q\right)g_3(u,p)\right]\mathrm{d}u = -\frac{D_0}{p}\mathrm{e}^{-\beta x}, \quad x\in(a,b), \tag{59}$$

$$\frac{1}{\pi}\int_a^b\left[f_{150}\left(\frac{1}{u-x}+Q\right)g_1(u,p) - g_{110}\left(\frac{1}{u-x}+Q\right)g_2(u,p) - \mu_{110}\left(\frac{1}{u-x}+Q\right)g_3(u,p)\right]\mathrm{d}u = -\frac{B_0}{p}\mathrm{e}^{-\beta x}, \quad x\in(a,b), \tag{60}$$

where

$$Q(u,x) = h_{12}(u,x) + \tilde{k}_{12}(u,x), \tag{61}$$

$$\tilde{k}_{11}(u,x,p) = \int_0^{\infty} [M(\alpha,u,x,p) + M(-\alpha,u,x,p) - \sin\alpha(u-x)]\,d\alpha, \tag{62}$$

$$\tilde{k}_{12}(u,x) = \int_0^{\infty} [N(\alpha,u,x) + N(-\alpha,u,x) - \sin\alpha(u-x)]\,d\alpha, \tag{63}$$

$$M = \frac{m_1}{2i\alpha} e^{i\alpha(u-x)}, \quad N = \frac{n_1}{2i\alpha} e^{i\alpha(u-x)}. \tag{64}$$

Introducing the following normalized quantities:

$$u = \eta(b-a)/2 + (b+a)/2, \quad x = \varsigma(b-a)/2 + (b+a)/2, \quad -1 < (\eta,\varsigma) < 1, \tag{65}$$

$$G_1(\eta,p) = g_1(u,p), \quad G_2(\eta,p) = g_2(u,p), \quad G_3(\eta,p) = g_3(u,p), \tag{66}$$

$$t_1(\varsigma) = -e^{-\beta x}\tau_0, \quad t_2(\varsigma) = -e^{-\beta x}D_0, \quad t_3(\varsigma) = -e^{-\beta x}B_0. \tag{67}$$

Eqs. (58)–(60) can be further written as

$$\begin{aligned}\frac{1}{\pi}\int_{-1}^{1}\left(\frac{1}{\eta-\varsigma} + \widehat{Q}(\eta,\varsigma)\right)(c_{440}G_1(\eta,p) + e_{150}G_2(\eta,p) + f_{150}G_3(\eta,p))\,d\eta \\ + \frac{1}{\pi}\int_{-1}^{1} m_{10}\left(\hat{h}_{11}(\eta,\varsigma,p) + \hat{\tilde{k}}_{11}(\eta,\varsigma,p) - \widehat{Q}(\eta,\varsigma)\right)G_1(\eta,p)\,d\eta = \frac{t_1(\varsigma)}{p},\end{aligned} \tag{68}$$

$$\frac{1}{\pi}\int_{-1}^{1}\left(\frac{1}{\eta-\varsigma} + \widehat{Q}(\eta,\varsigma)\right)(e_{150}G_1(\eta,p) - \varepsilon_{110}G_2(\eta,p) - g_{110}G_3(\eta,p))\,d\eta = \frac{t_2(\varsigma)}{p}, \tag{69}$$

$$\frac{1}{\pi}\int_{-1}^{1}\left(\frac{1}{\eta-\varsigma} + \widehat{Q}(\eta,\varsigma)\right)(f_{150}G_1(\eta,p) - g_{110}G_2(\eta,p) - \mu_{110}G_3(\eta,p))\,d\eta = \frac{t_3(\varsigma)}{p}, \tag{70}$$

where

$$\widehat{Q}(\eta,\varsigma) = \frac{b-a}{2}Q(u,x), \tag{71a}$$

$$\hat{h}_{11}(\eta,\varsigma,p) = \frac{b-a}{2}h_{11}(u,x,p), \quad \hat{\tilde{k}}_{11}(\eta,\varsigma,p) = \frac{b-a}{2}\tilde{k}_{11}(u,x,p) \tag{71b}$$

and the single-valued conditions (22) may be expressed as

$$\int_{-1}^{1} G_1(\eta,p)\,d\eta = 0, \quad \int_{-1}^{1} G_2(\eta,p)\,d\eta = 0, \quad \int_{-1}^{1} G_3(\eta,p)\,d\eta = 0. \tag{72}$$

Based on the numerical method of Erdogan and Gupta (1972), a system of linear algebraic equations can be obtained as

$$\begin{aligned}\sum_{j=1}^{K}\left(\frac{1}{\eta_j-\varsigma_i} + \widehat{Q}(\eta_j,\varsigma_i)\right)\frac{c_{440}R_1(\eta_j,p) + e_{150}R_2(\eta_j,p) + f_{150}R_3(\eta_j,p)}{K} \\ + \sum_{j=1}^{K} m_{10}\left(\hat{h}_{11}(\eta_j,\varsigma_i,p) + \hat{\tilde{k}}_{11}(\eta_j,\varsigma_i,p) - \widehat{Q}(\eta_j,\varsigma_i)\right)\frac{R_1(\eta_j,p)}{K} = \frac{t_1(\varsigma_i)}{p},\end{aligned} \tag{73}$$

$$\sum_{j=1}^{K}\left(\frac{1}{\eta_j-\varsigma_i} + \widehat{Q}(\eta_j,\varsigma_i)\right)\frac{e_{150}R_1(\eta_j,p) - \varepsilon_{110}R_2(\eta_j,p) - g_{110}R_3(\eta_j,p)}{K} = \frac{t_2(\varsigma_i)}{p}, \tag{74}$$

$$\sum_{j=1}^{K}\left(\frac{1}{\eta_j-\varsigma_i}+\widehat{Q}(\eta_j,\varsigma_i)\right)\frac{f_{150}R_1(\eta_j,p)-g_{110}R_2(\eta_j,p)-\mu_{110}R_3(\eta_j,p)}{K}=\frac{t_3(\varsigma_i)}{p}, \tag{75}$$

$$\sum_{j=1}^{K}R_1(\eta_j,p)/K=0, \tag{76}$$

$$\sum_{j=1}^{K}R_2(\eta_j,p)/K=0, \tag{77}$$

$$\sum_{j=1}^{K}R_3(\eta_j,p)/K=0, \tag{78}$$

where

$$R_1=\sqrt{1-\eta^2}G_1(\eta,p),\quad R_2=\sqrt{1-\eta^2}G_2(\eta,p),\quad R_3=\sqrt{1-\eta^2}G_3(\eta,p), \tag{79}$$

$$\eta_j=\cos[(2j-1)\pi/2K],\quad j=1,2,\ldots,K, \tag{80}$$

$$\varsigma_i=\cos(\mathrm{i}\pi/K),\quad i=1,2,\ldots,K-1. \tag{81}$$

K is the number of the discrete points of η.

4. Definition and analysis of field intensity factors and energy release rates

The dynamic stress intensity factors (DSIFs), dynamic electric displacement intensity factors (DEDIFs) and dynamic magnetic induction intensity factors (DMIIFs) in Laplace domain are defined as

$$K^*_{\mathrm{IIIa}}=\lim_{x\to a}\sqrt{2\pi(a-x)}\sigma^*_{yz}(x,0,p),\quad K^*_{\mathrm{IIIb}}=\lim_{x\to b}\sqrt{2\pi(x-b)}\sigma^*_{yz}(x,0,p), \tag{82}$$

$$K^*_{Da}=\lim_{x\to a}\sqrt{2\pi(a-x)}D^*_y(x,0,p),\quad K^*_{Db}=\lim_{x\to b}\sqrt{2\pi(x-b)}D^*_y(x,0,p), \tag{83}$$

$$K^*_{Ba}=\lim_{x\to a}\sqrt{2\pi(a-x)}B^*_y(x,0,p),\quad K^*_{Bb}=\lim_{x\to b}\sqrt{2\pi(x-b)}B^*_y(x,0,p). \tag{84}$$

Expanding $R_1(\eta, p)$, $R_2(\eta, p)$ and $R_3(\eta, p)$ in forms of Chebyshev polynomials $T_j(\eta)$ and applying the following property of $T_j(\eta)$

$$\frac{1}{\pi}\int_{-1}^{1}\frac{(1-\eta^2)^{-1/2}T_j(\eta)}{\eta-\varsigma}\,\mathrm{d}\eta=\frac{\left[(\varsigma^2-1)^{1/2}-\varsigma\right]^j}{(-1)^{j+1}(\varsigma^2-1)^{1/2}},\quad |\varsigma|>1, \tag{85}$$

we obtain

$$K^*_{\mathrm{IIIa}}=\mathrm{e}^{\beta a}\sqrt{\frac{b-a}{2}}\pi[c_{440}R_1(-1,p)+e_{150}R_2(-1,p)+f_{150}R_3(-1,p)], \tag{86a}$$

$$K^*_{\mathrm{IIIb}}=-\mathrm{e}^{\beta b}\sqrt{\frac{b-a}{2}}\pi[c_{440}R_1(1,p)+e_{150}R_2(1,p)+f_{150}R_3(1,p)], \tag{86b}$$

$$K^*_{Da}=\mathrm{e}^{\beta a}\sqrt{\frac{b-a}{2}}\pi[e_{150}R_1(-1,p)-\varepsilon_{110}R_2(-1,p)-g_{110}R_3(-1,p)], \tag{87a}$$

$$K^*_{Db}=-\mathrm{e}^{\beta b}\sqrt{\frac{b-a}{2}}\pi[e_{150}R_1(1,p)-\varepsilon_{110}R_2(1,p)-g_{110}R_3(1,p)], \tag{87b}$$

$$K^*_{Ba} = \mathrm{e}^{\beta a}\sqrt{\frac{b-a}{2}\pi}[f_{150}R_1(-1,p) - g_{110}R_2(-1,p) - \mu_{110}R_3(-1,p)], \tag{88a}$$

$$K^*_{Bb} = -\mathrm{e}^{\beta b}\sqrt{\frac{b-a}{2}\pi}[f_{150}R_1(1,p) - g_{110}R_2(1,p) - \mu_{110}R_3(1,p)]. \tag{88b}$$

Note Eqs. (76)–(78) can be written as

$$\sum_{j=1}^{K}\left[c_{440}R_1(\eta_j,p) + e_{150}R_2(\eta_j,p) + f_{150}R_3(\eta_j,p)\right] = 0, \tag{89}$$

$$\sum_{j=1}^{K}\left[e_{150}R_1(\eta_j,p) - \varepsilon_{110}R_2(\eta_j,p) - g_{110}R_3(\eta_j,p)\right] = 0, \tag{90}$$

$$\sum_{j=1}^{K}\left[f_{150}R_1(\eta_j,p) - g_{110}R_2(\eta_j,p) - \mu_{110}R_3(\eta_j,p)\right] = 0. \tag{91}$$

It is easy to know that $e_{150}R_1(\eta_j,p) - \varepsilon_{110}R_2(\eta_j,p) - g_{110}R_3(\eta_j,p)$ and $f_{150}R_1(\eta_j,p) - g_{110}R_2(\eta_j,p) - \mu_{110}R_3(\eta_j,p)$ are independent and that they respectively can be obtained by solving Eqs. (74) and (90), and Eqs. (75) and (91). By expressing the solution of Eqs. (74) and (90) for unit electrical loads as following

$$e_{150}R_1(\eta_j,p) - \varepsilon_{110}R_2(\eta_j,p) - g_{110}R_3(\eta_j,p) = \Phi(\eta_j)/p, \tag{92}$$

the DEDIFs and DMIIFs in time domain can be obtained from Eqs. (87)–(88) as

$$K_{Da} = \mathrm{e}^{\beta a}D_0\sqrt{\frac{b-a}{2}\pi}\Phi(-1)H(t), \quad K_{Db} = -\mathrm{e}^{\beta b}D_0\sqrt{\frac{b-a}{2}\pi}\Phi(1)H(t), \tag{93}$$

$$K_{Ba} = \mathrm{e}^{\beta a}B_0\sqrt{\frac{b-a}{2}\pi}\Phi(-1)H(t), \quad K_{Bb} = -\mathrm{e}^{\beta b}B_0\sqrt{\frac{b-a}{2}\pi}\Phi(1)H(t). \tag{94}$$

It can be seen that both the DEDIFs and DMIIFs are the Heaviside unit step function of time, and only related to the corresponding electrical or magnetical impact loads. They are both independent of the mechanical loads as well as the relevant material constants. This coincides with the results for the static problem.

With the solutions of $e_{150}R_1(\eta_j,p) - \varepsilon_{110}R_2(\eta_j,p) - g_{110}R_3(\eta_j,p)$ and $f_{150}R_1(\eta_j,p) - g_{110}R_2(\eta_j,p) - \mu_{110}R_3(\eta_j,p)$, $c_{440}R_1(-1,p) + e_{150}R_2(-1,p) + f_{150}R_3(-1,p)$ can be obtained from Eqs. (73) and (89). The DSIFs in time domain can be written as

$$K_{\mathrm{IIIa}} = \mathrm{e}^{\beta a}\sqrt{\frac{b-a}{2}\pi}\Psi(-1,t), \quad K_{\mathrm{IIIb}} = -\mathrm{e}^{\beta b}\sqrt{\frac{b-a}{2}\pi}\Psi(1,t), \tag{95}$$

where

$$\Psi(\eta,t) = \frac{1}{2\pi\mathrm{i}}\int_{Br}[c_{440}R_1(\eta,p) + e_{150}R_2(\eta,p) + f_{150}R_3(\eta,p)]\mathrm{e}^{pt}\,\mathrm{d}p. \tag{96}$$

It is easy to know that the DSIFs are related to mechanical loads, electrical loads, magnetical loads and the relevant material constants. However, when the loads tend to be static ones, $\hat{h}_{11}(\eta_j,\varsigma_i,p) + \hat{\hat{k}}_{11}(\eta_j,\varsigma_i,p) - \widehat{Q}(\eta_j,\varsigma_i)$ in Eq. (73) vanishes, the resulting SIFs will become, from Eqs. (73) and (89), as follows

$$K_{\mathrm{IIIa}} = \mathrm{e}^{\beta a}\tau_0\sqrt{\frac{b-a}{2}\pi}\Phi(-1)H(t), \quad K_{\mathrm{IIIb}} = -\mathrm{e}^{\beta b}\tau_0\sqrt{\frac{b-a}{2}\pi}\Phi(1)H(t). \tag{97}$$

That is, for static problem, the SIFs are only related to mechanical loads as well.

It should be noted that if all the magnetic quantities are made to vanish, the magneto-electro-elastic solution reduces to the dynamic anti-plane crack problem of piezoelectric material (Chen and Yu, 1997). This means our results are universal and correct.

Further extending the traditional concept of dynamic stress intensity factor to the dynamic strain intensity factor K_S, electric field intensity factor K_E and magnetic field intensity factor K_H, we have from Eqs. (95), (93), (94) and (1), (2), (3)

$$\begin{pmatrix} K_{Sa} \\ K_{Ea} \\ K_{Ha} \end{pmatrix} = \lim_{x\to a}\sqrt{2\pi(a-x)}\begin{pmatrix} w_{,y}(x,0,t) \\ -\phi_{,y}(x,0,t) \\ -\psi_{,y}(x,0,t) \end{pmatrix} = \sqrt{\frac{b-a}{2}}\pi\Pi^{-1}\begin{pmatrix} \Psi(-1,t)d \\ D_0\Phi(-1)H(t) \\ B_0\Phi(-1)H(t) \end{pmatrix}, \tag{98}$$

$$\begin{pmatrix} K_{Sb} \\ K_{Eb} \\ K_{Hb} \end{pmatrix} = \lim_{x\to b}\sqrt{2\pi(x-b)}\begin{pmatrix} w_{,y}(x,0,t) \\ -\phi_{,y}(x,0,t) \\ -\psi_{,y}(x,0,t) \end{pmatrix} = -\sqrt{\frac{b-a}{2}}\pi\Pi^{-1}\begin{pmatrix} \Psi(1,t) \\ D_0\Phi(1)H(t) \\ B_0\Phi(1)H(t) \end{pmatrix}, \tag{99}$$

where

$$\Pi = \begin{pmatrix} c_{440} & -e_{150} & -f_{150} \\ e_{150} & \varepsilon_{110} & g_{110} \\ f_{150} & g_{110} & \mu_{110} \end{pmatrix}. \tag{100}$$

Obviously, K_S, K_E and K_H all depend on material constants and applied loads including mechanical loads, electrical loads and magnetical loads.

For the magneto-electrically impermeable cracks, as the electrical and/or magnetical impacts are loaded, the DSIFs cannot perfectly reflect the fracture characteristics as in the purely elastic case. Therefore, the dynamic energy release rates (DERRs) G are introduced by calculating the work done in closing the crack tip over an infinitesimal distance. In accordance with the definition of the energy release rate proposed by Pak (1990), after a similar deriving process carried out by Wang and Yu (2000), we can finally obtain

$$G_\Xi(t) = \frac{1}{2}\left[K_{\mathrm{III}\Xi}(t)\widetilde{K}_{w\Xi}(t) + K_{D\Xi}(t)\widetilde{K}_{\phi\Xi}(t) + K_{B\Xi}(t)\widetilde{K}_{\psi\Xi}(t)\right], \quad \Xi = a, b, \tag{101}$$

where

$$\widetilde{K}_{w\Xi} = \frac{(\mu_{110}\varepsilon_{110} - g_{110}^2)K_{\mathrm{III}\Xi} + (e_{150}\mu_{110} - f_{150}g_{110})K_{D\Xi} + (f_{150}\varepsilon_{110} - e_{150}g_{110})K_{B\Xi}}{(c_{440}\mu_{110}\varepsilon_{110} + e_{150}^2\mu_{110} + f_{150}^2\varepsilon_{110} - c_{440}g_{110}^2 - 2e_{150}f_{150}g_{110})\mathrm{e}^{\beta\Xi}}, \tag{102a}$$

$$\widetilde{K}_{\phi\Xi} = \frac{(e_{150}\mu_{110} - f_{150}g_{110})K_{\mathrm{III}\Xi} - (c_{440}\mu_{110} + f_{150}^2)K_{D\Xi} + (c_{440}g_{110} + e_{150}f_{150})K_{B\Xi}}{(c_{440}\mu_{110}\varepsilon_{110} + e_{150}^2\mu_{110} + f_{150}^2\varepsilon_{110} - c_{440}g_{110}^2 - 2e_{150}f_{150}g_{110})\mathrm{e}^{\beta\Xi}}, \tag{102b}$$

$$\widetilde{K}_{\psi\Xi} = \frac{(f_{150}\varepsilon_{110} - e_{150}g_{110})K_{\mathrm{III}\Xi} + (c_{440}g_{110} + e_{150}f_{150})K_{D\Xi} - (c_{440}\varepsilon_{110} + e_{150}^2)K_{B\Xi}}{(c_{440}\mu_{110}\varepsilon_{110} + e_{150}^2\mu_{110} + f_{150}^2\varepsilon_{110} - c_{440}g_{110}^2 - 2e_{150}f_{150}g_{110})\mathrm{e}^{\beta\Xi}}. \tag{102c}$$

For magneto-electrically permeable case, the singular integral equation and the single-valued condition can be derived by a similar method as

$$\frac{1}{\pi}\int_a^b \left[m_{10}(h_{11} + \tilde{k}_{11} - Q) + c_{440}\left(\frac{1}{u-x} + Q\right)\right]g_1(u,p)\,\mathrm{d}u = -\frac{\tau_0}{p}\mathrm{e}^{-\beta x}, \quad x \in (a,b), \tag{103}$$

$$\int_a^b g_1(u,p)\,\mathrm{d}u = 0. \tag{104}$$

The electric displacement $D_y^*(x,0,p)$ and magnetic induction $B_y^*(x,0,p)$ on the crack surfaces can be obtained as

$$D_y^*(x,0,p) = e^{\beta x}\frac{1}{\pi}\int_a^b e_{150}\left(\frac{1}{u-x}+Q(u,x)\right)g_1(u,p)\,du - \frac{D_0}{p}, \quad x\in(a,b), \tag{105}$$

$$B_y^*(x,0,p) = e^{\beta x}\frac{1}{\pi}\int_a^b f_{150}\left(\frac{1}{u-x}+Q(u,x)\right)g_1(u,p)\,du - \frac{B_0}{p}, \quad x\in(a,b), \tag{106}$$

The field intensity factors and DERRs in time domain are respectively

$$K_{\text{IIIa}} = e^{\beta a}\sqrt{\frac{b-a}{2}}\pi c_{440}R_1(-1,t), \quad K_{\text{IIIb}} = -e^{\beta b}\sqrt{\frac{b-a}{2}}\pi c_{440}R_1(1,t), \tag{107}$$

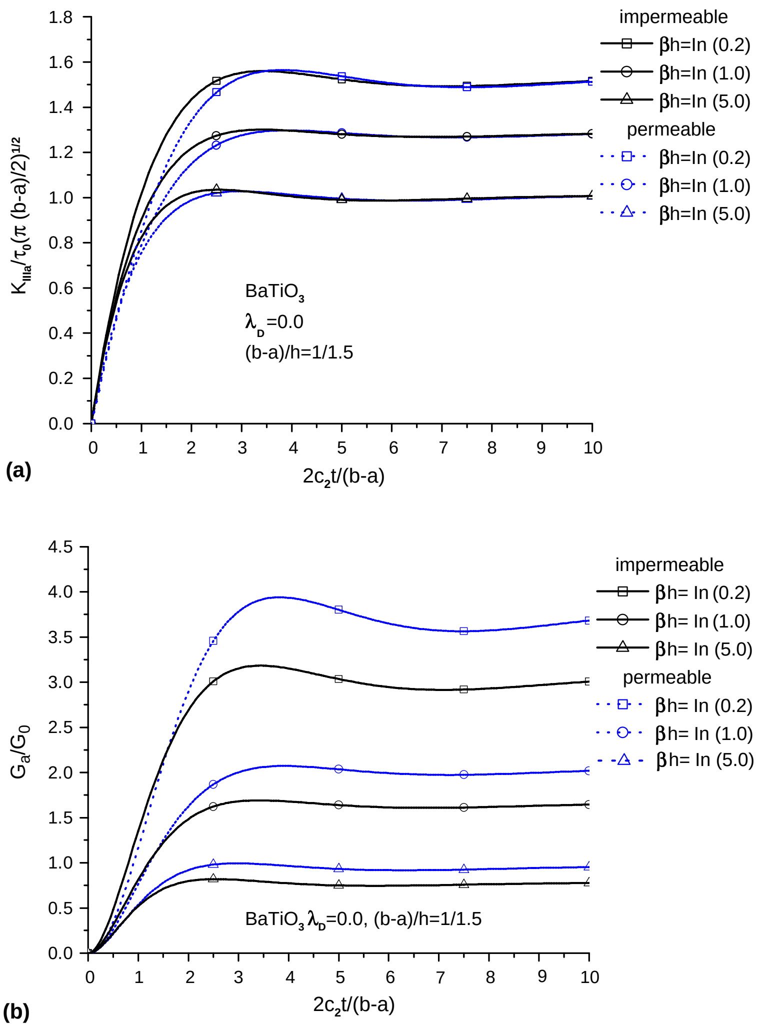

Fig. 2. Comparison of normalized (a) DSIFs and (b) DERRs between electrically impermeable and permeable cracks under shear impacts for functionally graded piezoelectric strip.

$$K_{Da} = \frac{e_{150}}{c_{440}} K_{\mathrm{III}a}(t), \quad K_{Db} = \frac{e_{150}}{c_{440}} K_{\mathrm{III}b}(t), \tag{108}$$

$$K_{Ba} = \frac{f_{150}}{c_{440}} K_{\mathrm{III}a}(t), \quad K_{Bb} = \frac{f_{150}}{c_{440}} K_{\mathrm{III}b}(t), \tag{109}$$

$$K_{Sa} = \frac{1}{c_{440\mathrm{e}^{\beta a}}} K_{\mathrm{III}a}(t), \quad K_{Sb} = \frac{1}{c_{440\mathrm{e}^{\beta b}}} K_{\mathrm{III}b}(t), \tag{110}$$

$$K_{Ea} = K_{Eb} = 0, \tag{111}$$

$$K_{Ha} = K_{Hb} = 0, \tag{112}$$

$$G_a = \frac{K^2_{\mathrm{III}a}(t)}{2c_{440}} \mathrm{e}^{-\beta a}, \quad G_b = \frac{K^2_{\mathrm{III}b}(t)}{2c_{440}} \mathrm{e}^{-\beta b}, \tag{113}$$

where

$$R_1(\eta, t) = \frac{1}{2\pi \mathrm{i}} \int_{Br} R_1(\eta, p) \mathrm{e}^{pt} \, \mathrm{d}p, \tag{114}$$

and $R_1(\eta, p)$ can be obtained by solving Eqs. (103) and (104).

As shown in Eqs. (107)–(113), for magneto-electrically permeable cracks, both the electric field intensity factors and magnetic field intensity factors vanish. Electrical loads and magnetical loads reduce the concentration of DEDIFs and DMIIFs, respectively. Material graded index has the same influences on the DSIFs, DEDIFs, DMIIFs and dynamic strain intensity factors. The DERRs, DEDIFs, DMIIFs and dynamic strain intensity factors are the functions of the DSIFs, and all of them including the DSIFs depend on not only shear loads but also material parameters. Both imposed magnetical loads and electrical loads do not contribute to the DSIFs and/or DERRs, thus, the DERRs and DSIFs are quite equivalent to be a fracture parameter. This is similar to the electrically permeable crack problem of piezoelectric materials (Wang and Yu, 2000). In the absence of the mechanical impact loads, in other words, the material is in effect seamless as far as both the electric field and the magnetic field are concerned, and the fields will not be perturbed by the presence of the cracks (McMeeking, 1989). It should also be noted that when the loads tend to static ones, $m_{10}(h_{11} + \tilde{k}_{11} - Q)$ in Eq. (103) vanishes, the SIFs will be quite in agreement

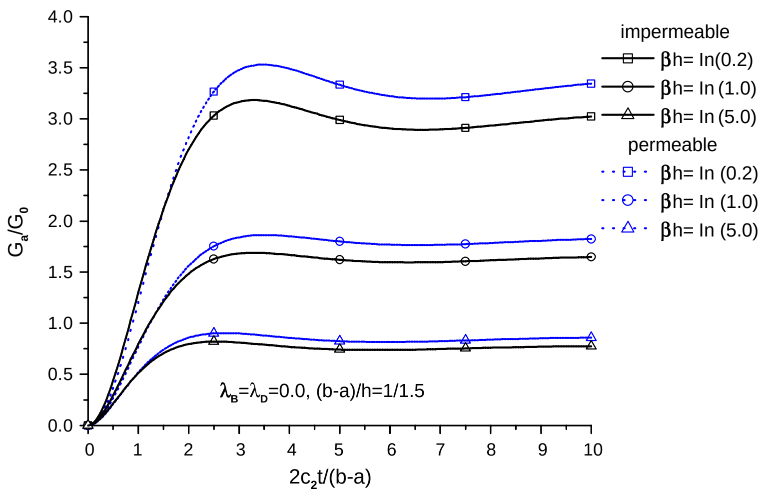

Fig. 3. Comparison of normalized DERRs between magneto-electrically impermeable and permeable cracks under shear impacts for functionally graded magneto-electro-elastic strip.

with the magneto-electrically impermeable case, i.e., Eq. (97). This means for static problem, the SIFs are related to the shear loads only.

5. Numerical results and discussion

In this section, we investigate the responses of functionally graded magneto-electro-elastic strip with a central crack ($b + a = h$). Since the DERRs and field intensity factors at the left crack tip for a certain material gradient parameter βh have definite relations to those at the right crack tip for the corresponding negative value $-\beta h$, only the numerical results at the left crack tip will be presented. Without any loss in generality, in all our numerical procedure, τ_0 is taken as 4.2×10^6 N/m^2.

For comparison with the known results, as a special example, the DSIFs and DERRs for the crack problem of functionally graded piezoelectric material under both electrically impermeable and electrically permeable crack surface conditions are first calculated. The material constants at $x = 0$ plane are assumed

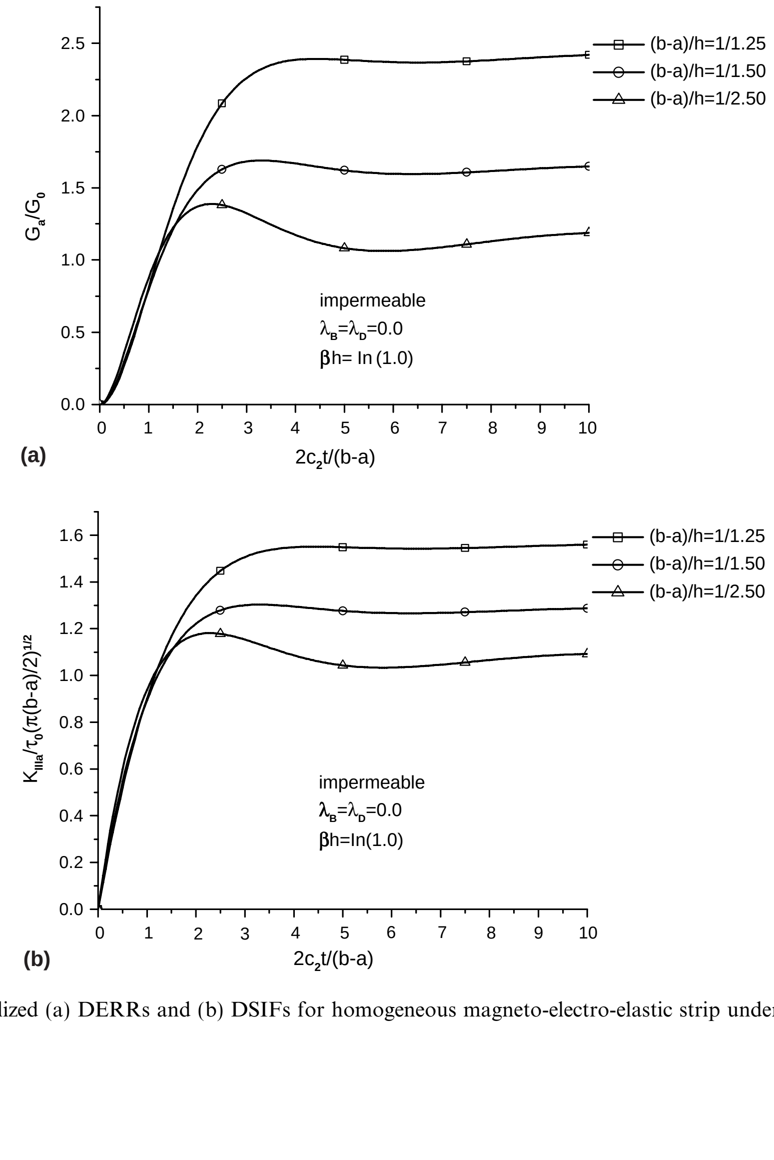

Fig. 4. Normalized (a) DERRs and (b) DSIFs for homogeneous magneto-electro-elastic strip under shear impacts.

to be those of $BaTiO_3$ (Wang and Yu, 2000; Chen et al., 2003). From the numerical results plotted in Fig. 2a, it is obvious that the present results are in good agreement with those given by Chen et al. (2003). From Fig. 2b, where $G_0 = \pi(b-a)\tau_0^2/[4(c_{440} + e_{150}^2/\varepsilon_{110})]$, it is found that for homogeneous piezoelectric strip, i.e., $\beta h = \text{In}(1.0)$, our results are also in agreement with those given by Wang and Yu (2000).

For functionally graded magneto-electro-elastic material, for the sake of generality, the material constants at $x = 0$ plane are taken as (Song and Sih, 2003)

$$c_{440} = 44.65 \times 10^9\ \text{N/m}^2, \quad e_{150} = 5.7\ \text{C/m}^2, \quad \varepsilon_{110} = 6.46 \times 10^{-9}\ \text{C/V m},$$
$$f_{150} = 275.0\ \text{N/A m}, \quad \mu_{110} = -292.5 \times 10^{-6}\ \text{N s}^2/\text{C}^2, \quad \rho_0 = 6.49 \times 10^3\ \text{kg/m}^3,$$

i.e., in Eq. (A.1) in Song and Sih (2003), the composite is assumed to be made of $BaTiO_3$ as the inclusions and $CoFe_2O_4$ as the matrix, and the volume fraction of the inclusions is taken as $V_f = 0.5$. Numerical

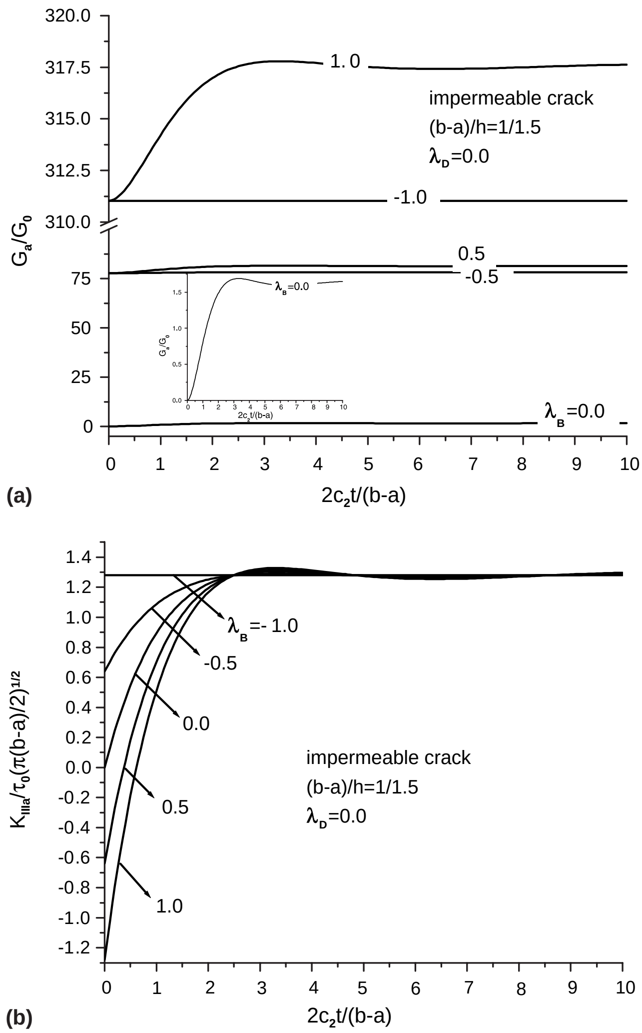

Fig. 5. Normalized (a) DERRs and (b) DSIFs for functionally graded magneto-electro-elastic strip under various magnetical loads as $\lambda_D = 0.0$.

results are presented in Figs. 3–8, where the DERRs are normalized by G_0 which is determined as $G_0 = \pi(b-a)\tau_0^2/(4\mu_0)$. The loading combination parameter λ_B is determined as $\lambda_B = B_0 f_{150}/(\tau_0\mu_{110})$ which is used to reflect the combination between the mechanical impact $-\tau_0 H(t)$ and the magnetical impact $-B_0 H(t)$. λ_D is determined as $\lambda_D = D_0 e_{150}/(\tau_0\varepsilon_{110})$ which is used to reflect the combination between the mechanical impact $-\tau_0 H(t)$ and the electrical impact $-D_0 H(t)$.

Fig. 3 compares the normalized DERRs between the magneto-electrically impermeable and permeable cases for $(b-a)/h = 1/1.5$ in the absence of magneto-electrical impacts ($\lambda_B = \lambda_D = 0$). The peak value corresponding to magneto-electrically impermeable cracks are smaller than that corresponding to permeable cracks. There are no other distinct differences. Since both magnetical and electrical impacts have no contribution to the DERRs and/or DSIFs for the magneto-electrically permeable cracks, the following part of this section will mainly concentrate on the impermeable case.

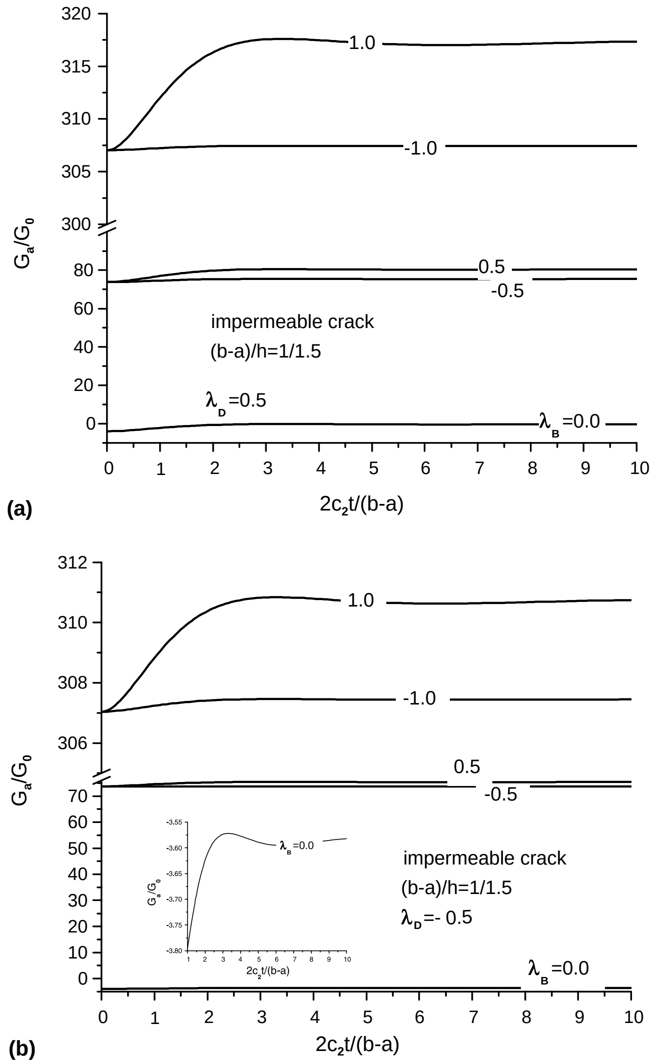

Fig. 6. Normalized DERRs for functionally graded magneto-electro-elastic strip under various magnetical loads as (a) $\lambda_D = 0.5$, (b) $\lambda_D = -0.5$.

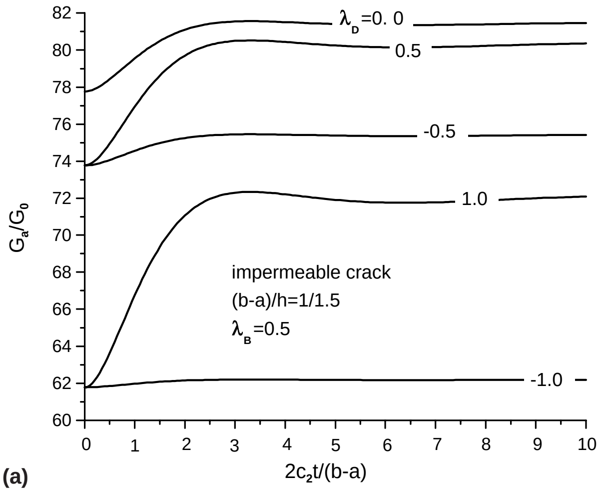

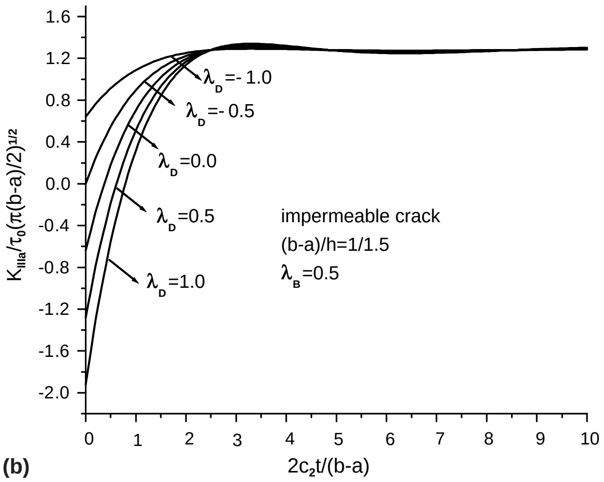

Fig. 7. Normalized (a) DERRs and (b) DSIFs for functionally graded magneto-electro-elastic strip under various electrical loads as $\lambda_B = 0.5$.

For the homogeneous magneto-electro-elastic strip, the DERRs and DSIFs under the shear impacts are plotted in Fig. 4. As shown in Fig. 4, the peak values of DERRs or DSIFs will increase with the increasing of $(b - a)/h$, and the DERRs and DSIFs are also equivalent to be a fracture parameter under only mechanical impacts, which is similar to electrically impermeable crack problem of piezoelectric materials (Wang and Yu, 2000).

Figs. 5 and 6 show that for definite electrical loads, in general, magnetical loads enhance crack propagation and growth, and that positive magnetical loads effectively enhance crack propagation compared with negative magnetical loads. Figs. 5 and 6 also indicate that for definite electrical impact loads, at $t = 0$, the DERRs for a fixed λ_B equal to that for corresponding $-\lambda_B$.

Fig. 7 shows that for definite magnetical loads, electrical loads always decrease the DERRs, and that negative electrical loads are easier to inhibit crack growth than positive electrical loads. In addition, for definite magnetical loads, at $t = 0$, the DERRs for a fixed λ_D equal to that for $-\lambda_D$ as well. This coincides with electrically impermeable crack problem for homogeneous piezoelectric strip (Wang and Yu, 2000).

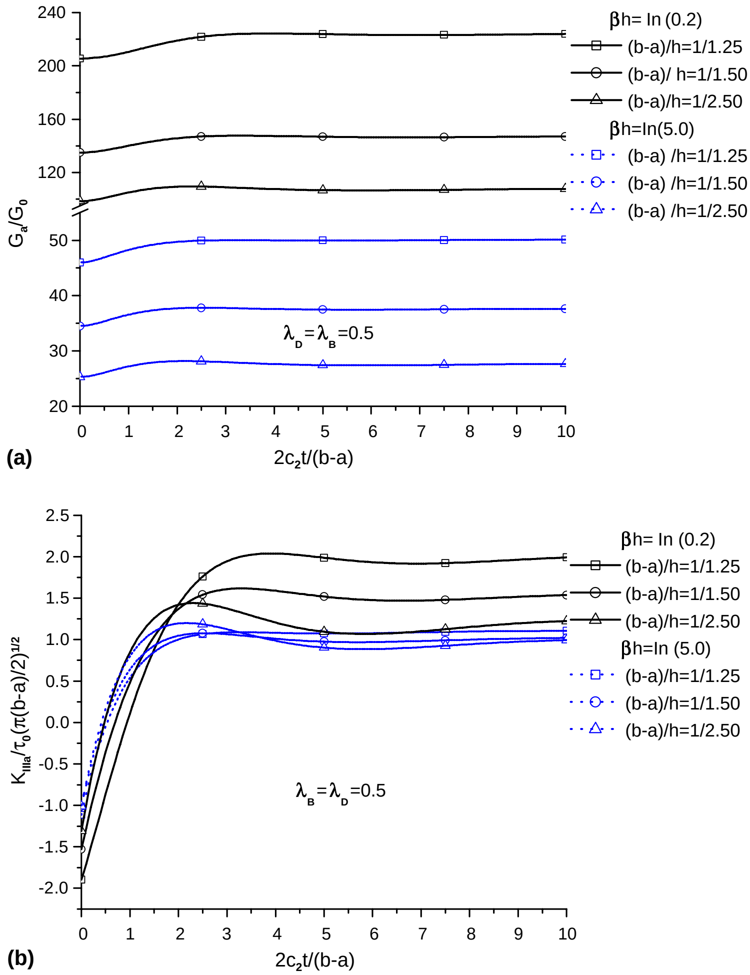

Fig. 8. Effects of $(b-a)/h$ and βh on normalized (a) DERRs and (b) DSIFs for functionally graded magneto-electro-elastic strip.

Fig. 8 shows the effects of crack size $(b-a)/h$ and material gradient parameter βh on the normalized DERRs and DSIFs. It is found that the maximum of DERRs and/or DSIFs at the left crack tip will increase as $(b-a)/h$ increases or βh decreases. And with the increase of βh, the effect of $(b-a)/h$ on the normalized DERR and/or DSIF will decrease.

6. Conclusions

(1) Integral transform and singular integral equation method can be used effectively to solve the dynamic response of a functionally graded magneto-electro-elastic strip containing a finite crack subjected to magneto-electro-mechanical impacts.
(2) For the magneto-electrically impermeable cracks, the DEDIFs and DMIFs are, respectively, related to applied electrical loads and magnetical loads only. All the other field intensity factors and DERRs depend on both applied loads including mechanical, electrical and magnetical loads and material parameters. In addition, both DEDIFs and DMIFs are the Heaviside step function of time.

(3) For the magneto-electrically permeable cracks, both magnetical and electrical impacts have no contribution to the DERR and field intensity factors. Both magnetic field and electric field intensity factors vanish. All other field intensity factors and DERRs are related to mechanical loads and material parameters. Among others, only one of them, such as stress intensity factor, is independent.
(4) In general, the maximum of normalized DERRs for magneto-electrically permeable cracks are generally higher than that for impermeable case under only mechanical impacts.
(5) For the magneto-electrically impermeable cracks, the loading combination parameters have significant and different influences on the normalized DERRs and DSIFs. According to maximum energy release rate criterion, magnetical loads always enhance the crack propagation, and the cracks are easier to propagate under positive magnetical loads than under negative magnetical loads. However, electric displacement loads always impede the crack propagation, and the negative electrical loads effectively inhibit crack propagation compared with positive electrical loads.
(6) For both magneto-electrically impermeable and permeable cracks, the increasing of material gradient parameter βh, in general, retards the crack extension.

Acknowledgements

The work was supported by the University Research Grant, The University of Hong Kong (small project funding 2004–2005) and the National Natural Science Fund of China (Project No. 10472074).

Appendix A

d_1, e_1, f_1, d_2, e_2 and f_2 in Eq. (11) are as follows:

$$d_1 = \frac{e_{150}\mu_{110} - f_{150}g_{110}}{\mu_{110}\varepsilon_{110} - g_{110}^2}, \quad e_1 = \frac{-\mu_{110}}{\mu_{110}\varepsilon_{110} - g_{110}^2}, \quad f_1 = \frac{g_{110}}{\mu_{110}\varepsilon_{110} - g_{110}^2}, \tag{A.1}$$

$$d_2 = \frac{\varepsilon_{110}f_{150} - e_{150}g_{110}}{\mu_{110}\varepsilon_{110} - g_{110}^2}, \quad e_2 = \frac{g_{110}}{\mu_{110}\varepsilon_{110} - g_{110}^2}, \quad f_2 = \frac{-\varepsilon_{110}}{\mu_{110}\varepsilon_{110} - g_{110}^2}. \tag{A.2}$$

m_{10}, m_{20}, m_{30} in Eq. (16) are as follows:

$$m_{10} = c_{440} + \frac{\varepsilon_{110}f_{150}^2 - 2e_{150}f_{150}g_{110} + \mu_{110}e_{150}^2}{\mu_{110}\varepsilon_{110} - g_{110}^2}, \quad m_{20} = \frac{f_{150}g_{110} - e_{150}\mu_{110}}{\mu_{110}\varepsilon_{110} - g_{110}^2}, \tag{A.3}$$

$$m_{30} = \frac{e_{150}g_{110} - f_{150}\varepsilon_{110}}{\mu_{110}\varepsilon_{110} - g_{110}^2}. \tag{A.4}$$

Appendix B

h_{1i}, $\tilde{h}_{1i}$ $(i = 1, 2)$ in Eqs. (55)–(57) are as follows:

$$\begin{aligned} h_{11}(u,x,p) = &\int_0^\infty \frac{2\mathrm{e}^{m_3x}}{m_3(\mathrm{e}^{m_3h} - \mathrm{e}^{m_2h})}\left[F_4(\alpha,u,p) - \mathrm{e}^{m_2h}F_1(\alpha,u,p)\right]\alpha\,\mathrm{d}\alpha \\ &+ \int_0^\infty \frac{2\mathrm{e}^{m_2x}}{m_2(\mathrm{e}^{m_2h} - \mathrm{e}^{m_3h})}\left[F_4(\alpha,u,p) - \mathrm{e}^{m_3h}F_1(\alpha,u,p)\right]\alpha\,\mathrm{d}\alpha \end{aligned} \tag{B.1}$$

$$h_{12}(u,x) = \int_0^\infty \frac{2e^{n_3 x}}{n_3(e^{n_3 h} - e^{n_2 h})}[F_5(\alpha,u) - e^{n_2 h}F_2(\alpha,u)]\alpha\,d\alpha + \int_0^\infty \frac{2e^{n_2 x}}{n_2(e^{n_2 h} - e^{n_3 h})}[F_5(\alpha,u) - e^{n_3 h}F_2(\alpha,u)]\alpha\,d\alpha \tag{B.2}$$

$$\tilde{h}_{11}(u,x,p) = \int_{-\infty}^{\infty} \frac{m_1}{2i\alpha} e^{i\alpha(u-x)}\,d\alpha, \tag{B.3}$$

$$\tilde{h}_{12}(u,x) = \int_{-\infty}^{\infty} \frac{n_1}{2i\alpha} e^{i\alpha(u-x)}\,d\alpha. \tag{B.4}$$

References

Avellaneda, M., Harshe, G., 1994. Magnetoelectric effect in piezoelectric/magnetostrictive multiplayer (2-2) composites. J. Intell. Mater. Syst. Struct. 5, 501–513.

Benveniste, Y., 1995. Magneto-electric effect in fibrous composites with piezoelectric and piezomagnetic phases. Phys. Rev. B B51, 16424–16427.

Buchanan, G.R., 2003. Free vibration of an infinite magneto-electro-elastic cylinder. J. Sound Vib. 268, 413–426.

Chen, J., Liu, Z.X., Zou, Z.Z., 2003. The central crack problem for a functionally graded piezoelectric strip. Int. J. Fract. 121, 81–94.

Chen, Z.T., Yu, S.W., 1997. Anti-plane dynamic fracture mechanics in piezoelectric materials. Int. J. Fract. 85, L3–L12.

Du, J.K., Shen, Y.P., Ye, D.Y., Yue, F.R., 2004. Scattering of anti-plane shear waves by a partially debonded magneto-electro-elastic circular cylindrical inhomogeneity. Int. J. Engng. Sci. 42, 887–913.

Erdogan, F., Gupta, G.D., 1972. On the numerical solution of singular integral equations. Quart. Appl. Math. 29, 525–539.

Gu, B., Yu, S.W., Feng, X.Q., 2002. Transient response of an insulating crack between dissimilar piezoelectric layers under mechanical and electrical impacts. Arch. Appl. Mech. 72, 615–629.

Harshe, G., Dougherty, J.P., Newnham, R.E., 1993. Theoretical modeling of 3-0/0-3 magnetoelectric composites. Int. J. Appl. Electromagn. Mater. 4, 161–171.

Hou, P.F., Leung, A.Y.T., 2004. The transient responses of magneto-electro-elastic hollow cylinders. Smart Mater. Struct. 13, 762–776.

Huang, J.H., Kuo, W.S., 1997. The analysis of piezoelectric/piezomagnetic composite materials containing an ellipsoidal inhomogeneity. J. Appl. Phys. 81, 1378–1386.

Kwon, S.M., Lee, K.Y., 2000. Transient response of a rectangular medium with a center crack. Eur. J. Mech. A/Solids 20, 457–468.

Lage, R.G., Soares, C.M.M., Soares, C.A.M., Reddy, J.N., 2004. Layerwise partial mixed finite element analysis of magneto-electro-elastic plates. Comput. Struct. 82, 1293–1301.

Li, J.Y., 2000. Magnetoelectroelastic multi-inclusion and inhomogeneity problems and their applications in composite materials. Int. J. Engng. Sci. 38, 1993–2011.

Li, X., 2001. Transient response of a piezoelectric material with a semi-infinite mode III crack under impact loads. Int. J. Fract. 111, 119–130.

Li, J.Y., Dunn, M.L., 1998. Micromechanics of magneto-electro-elastic composite materials: average fields and effective behavior. J. Intell. Mater. Syst. Struct. 9, 404–416.

McMeeking, R., 1989. On mechanical stress at cracks in dielectrics with application to dielectric breakdown. J. Appl. Phys. 62, 3116–3122.

Nan, C.W., 1994. Magneto-electric effect in composites of piezoelectric and piezomagnetic phases. Phys. Rev. B B50, 6082–6088.

Pak, Y.E., 1990. Crack extension force in a piezoelectric material. J. Appl. Mech. 57, 647–653.

Pan, E., 2001. Exact solution for simply supported and multilayered magneto-electro-elastic plates. ASME J. Appl. Mech. 68, 608–618.

Shindo, Y., Katsura, H., Yan, W., 1996. Dynamic stress intensity factor of a cracked electric medium in an uniform electric field. Acta Mech. 117, 1–10.

Sih, G.C., Song, Z.F., 2003. Magnetic and electric poling effects associated with crack growth in $BaTiO_3$-$CoFe_2O_4$ composite. Theor. Appl. Fract. Mech. 39, 209–227.

Song, Z.F., Sih, G.C., 2003. Crack initiation behavior in magnetoelectroelastic composite under in-plane deformation. Theor. Appl. Fract. Mech. 39, 189–207.

Van Suchtelen, J., 1972. Product properties: a new application of composite materials. Phillips Res. Rep. 27, 28–37.

Wang, X.M., Shen, Y.P., 1996. The conservation laws and path-independent integrals for linear electro-magneto-elastic media with an application. Int. J. Solids Struct. 33, 865–878.

Wang, X.Y., Yu, S.W., 2000. Transient response of a crack in a piezoelectric strip objected to the mechanical and electrical impacts: mode III problem. Int. J. Solids Struct. 37, 5795–5808.

Wu, T.L., Huang, J.H., 2000. Closed-form solutions for the magnetoelectric coupling coefficients in fibrous composites with piezoelectric and piezomagnetic phases. Int. J. Solids Struct. 37, 2981–3009.

Zhou, Z.G., Wang, B., Sun, Y.G., 2004. Two collinear interface cracks in magneto-electro-elastic composites. Int. J. Engng. Sci. 42, 1155–1167.